Nonlinear Optical Properties of Zwitterionic Merocyanine Aggregates: Role of Intermolecular Interaction and Solvent Polarity

Zuhail Sainudeen and Paresh Chandra Ray*

Department of Chemistry, Jackson State University, Jackson, Mississippi 39217

Received: May 27, 2005; In Final Form: July 22, 2005

We present a time-dependent quantum-chemical analysis on merocyanine aggregates to understand the insight of the intermolecular interactions and to find the relationship between structural and collective nonlinear optical properties. The first hyperpolarizabilities are evaluated for monomer and aggregates of a series of zwitterionic merocyanine dyes, whose synthesis and formation of H and J type aggregates in solvents are reported recently in the literature (*J. Am. Chem. Soc.* **2002**, *124*, 9431). The molecular geometries are obtained via B3LYP/6-31G** (hybrid density-functional theory) optimization including PCM approach, while the dynamic NLO properties are calculated with the TD-DFT/SOS and ZINDO/CV method including solvent effects. It has been observed that the first hyperpolarizability changes tremendously as monomers undergo aggregation, and the magnitude of first hyperpolarizabilities highly depends on the nature of the aggregates. It is found that solvents play a remarkable role on the structure and first hyperpolarizabilities of merocyanine monomers and aggregates. Changing the solvent from low to high dielectric causes not only an increase in magnitude of β but also a change in sign, therefore passing through zero at intermediate dielectric. The importance of our results on the design of electrooptic materials have been discussed.

Introduction

Photonics is playing an ever-increasing role in our modern information society. It is gradually replacing the electron, the elementary particle in electronics. In recent years an intense worldwide effort has been focused on the research of design and development of organic conjugated materials with large optical nonlinearities due to their potential applications in various optical devices.[1−5] Materials with high nonlinear optical (NLO) activities are useful as electrooptic switching elements for telecommunication and optical information processing. For communication, the electron as carrier in a metallic conductor has been replaced by the photon in an optical fiber. Multiwavelength optical communication increases the capacity on an optical network by orders of magnitude over electronic communication. Though a variety of materials including inorganic, organometallic, and organic compounds have been studied for their NLO activity, maximum attention has been devoted to organic materials since organic materials have number of advantages over inorganic materials for electrooptic (EO) applications, such as (i) the fact that their dielectric constants and refractive indices are much smaller, (ii) polarizabilities are purely electronic and therefore faster, and also (iii) molecules are compatible with a polymer matrix. A large number of organic π-conjugated molecules have been investigated [1−8] in the last 20 years. The outcome of the results has helped to establish certain guidelines for molecular design to obtain good second order nonlinear optical materials. However, roughly more than 80% of all π-conjugated organic molecules crystallize in centrosymmetric space groups, therefore producing materials with no second-order bulk susceptibility $\chi(2)$. So although great progress has been made in optimizing the NLO properties of the isolated chromophores, research on the role of intermolecular interactions that determined the alignment of the chromophores in the device configurations is still in its infancy.

To overcome centrosymmetric crystallization problem, organic NLO chromophores incorporated into poled polymer system have shown significant potential advantages.[9−12] Devices based on electrooptic polymers [9−12] have indicated a performance that could perhaps exceed the expectation and current requirements of the optical communication industry. For device application, the chromophore must be present at high concentration (>5% by mass) in the polymer, where interchromophore interactions can modify their properties substantially. In the process of device development, materials based on well designed chromophores having large dipole-moment and excellent molecular hyperpolarizabilities, often failed to provide expected electrooptic response.[13−14] High dipole moments of the doping chromophores lead to strong intermolecular interaction and as a consequence formation of inactive aggregates at higher dye loading are common. A centrosymmetric (antiparallel) dimer structure can explain the discrepancies between the observed electrooptic effect of polymeric composite materials at high dye loading and the predicted effects based on molecular hyperpolarizability measurements in dilute solution. L. Dalton, T. J. Marks, and others[10,15−16] succeeded in providing experimental evidence that electrostatic intermolecular interaction between the dye molecules accounted the observed deficiencies in electrooptic coefficients. Clearly, the greatest uncertainties lie in crucial issues such as packing and intermolecular interaction acting to modify the polarization of the macroscopic sources.

The intermolecular interactions are sufficiently strong enough for the optical properties of the aggregates to differ from those of the corresponding monomer by a considerable amount. Many of the unique properties of the aggregate arise from the fact that the constituent molecules are strongly electronically coupled so that optical excitation of the chromophore produces a state that is delocalized over several monomer units. In addition, excitonic coupling between transient dipoles on neighboring chromophores will split the electronic transition into a broad

10.1021/jp052820+ CCC: $30.25
Published on Web 09/15/2005

band of state. This splitting can influence the magnitude of first hyperpolarizibality as well as the degree of optical transparency at the interested wavelength. The macroscopic photoactive properties such as absorption, emission, and nonlinear optical properties strongly depend on the interaction between the chromophores. According to the excitation theory,[17−18] the blue shift in the absorption spectra is due to the formation of H aggregates while the red shift is due to the J aggregate. An H aggregate is formed when dye molecules arrange themselves in a near vertical stack. A J aggregate is formed when the dye molecules arrange into a slanted stack. External environments can tune the formation of the different types of molecular aggregates. Many aggregates contain a large number of randomly or semirandomly positioned monomers encompassing a wide variety of different local interaction geometries, which creates a challenge for understanding the details of the role of intermolecular interaction for predicting linear and nonlinear optical properties of the aggregates.

Recent theoretical studies of Bella et al., Dutta et al., and others[19−22] have provided some insights into the effects of the intermolecular interactions on the first hyperpolarizabilties of *p*-nitroaniline (PNA), 2-methyl-4-nitroaniline (MNA), and 3-methyl-4-nitropyridine 1-oxide (POM) using semiempirical level of calculations. These chromophores are known to form aggregates mainly in crystals. In this work, we present a time-dependent ab initio molecular orbital calculation on merocyanine aggregates, aiming to investigate the insight of the intermolecular interactions and to understand the relationship between structural and collective optical properties. The primary reasons for the choice of merocyanine aggregates are as follows: (1) Merocyanine dyes are reported [23] to form only H aggregate in dioxane solvent even at 1 μM concentration and J aggregates have been shown to form when merocyanine dyes are incorporated in Langmuir Budget films.[24] Measurements of the first hyperpolarizabilities of J and H aggregates separately for merocyanine dyes using hyper-Rayleigh scattering[25,26] method are highly visible. (2) Due to the tunability of the π-system of merocyanines from weakly dipolar (polyenelike) to highly dipolar (zwitterionic) chromophores, merocyanines are identified as the most promising chromophores for NLO applications.[27−31] To design NLO devices, one must not only find simple molecules having large hyperpolarizabilities but also combine these molecules to form noncentrosymmetric macroscopic structures. This cannot be done without understanding the intermolecular interactions between those merocyanine chromophores. (3) Recently Cross et al.[32] have demonstrated by an electric field induced second harmonic generation (EFISHG)[33] experiment that the first hyperpolarizabilities of zwitterionic merocyanines change tremendously with aggregation. Not only did β values increase in magnitude but also a change in sign has been observed, and therefore, experimentally measured values pass through zero for the intermediate position of the aggregates. This drastic change in first hyperpolarizabilities with concentration triggered our interest in elucidating the structural and energetic origin of the strong intermolecular interaction between merocyanines in aggregates.

In this paper, we report a systematic study of the dynamic first hyperpolarizabilities of monomer and dimers of merocyanine dyes (Schemes 1 and 2) using time-dependent density functional theory (TD-DFT) [34,35] calculations with fairly extensive basis set (6-31G**). TD-DFT performs the calculations of frequency-dependent response properties like electronic excitations and frequency dependent hyperpolarizabilities. Several publications[7,8,36−37] have indicated that the calculated hyperpolarizabilities using the TD-DFT approach match very well with experimental trends. To understand how the solvent polarity affects the structure and NLO properties of the zwitterionic monomer and dimers of merocyanine dyes, we have used the self-consistent reaction field (SCRF) approach with the polarizable continuum model (PCM),[38,39] as implemented in Gaussian 03.[40] Recently Cammi [41] et al. and others[42,43] have used the polarizable continuum model to calculate the solvent effects on the hyperpolarizabilities of different chromophores. They have shown that the PCM model allows one to obtain complex NLO properties that can be directly compared with the outcome of the experimental measurements. Since it is not possible in this moment to calculate the dynamic β's for higher aggregates using the TD-DFT/SOS approach due to very high computational cost, here we have investigated the dynamic hyperpolarizabilities of higher aggregates using a combination of density functional theoretical (DFT) calculations with fairly extensive basis set [6-31G(d,p)] for geometry optimization and ZINDO/CV method for dynamic β calculations.

Computational Method

All the molecules reported in this paper have been fully optimized at the B3LYP (hybrid density-functional theory) ab initio levels with the 6-31G** basis set using the Gaussian 03 program. Synthesis of all the merocyanine dyes used in this paper have been reported before by Wurthner et al.[23] It is now well-known that the solvent polarity exerts an important influence on the structure as well as the first NLO coefficients in neutral and ionic molecules.[1−8] To explicitly take into account the solvent polarity effects, we have adapted the self-consistent reaction field (SCRF) approach with the polarizable continuum model (PCM) [38−43]as implemented in Gaussian 03. To account for both solvent and dispersion effects, we have adapted the TD-DFT/SOS (sum-over-state) approach with the SCRF/PCM method for the calculation of β's for monomer and dimers. The PCM is one of the most frequently used continuum solvation methods and has seen numerous variations over the years. The PCM calculates the molecular free energy in solution as the sum over three terms:

$$G_{sol} = G_{es} + G_{dr} + G_{cav} \quad (1)$$

These components represent the electrostatic (es) and the dispersion−repulsion (dr) contributions to the free energy and the cavitation energy (cav). All three terms are calculated using a cavity defined through interlocking van der Waals spheres centered at atomic positions. The reaction field is represented through point charges located on the surface of the molecular cavity. In the PCM approach, the partition between solute and solvent is performed by defining a cavity in the polarizable medium. The solute is placed inside the cavity, where the relative dielectric constant is 1 (i.e. the value of vacuum), while outside the dielectric constant has the macroscopic value of the solvent (for example 78.39 for water at 298 K, 10.36 for 1,2-dichloroethane, and so on). The shape and the size of the cavity are important parameters of this method. Polarizable continuum model constitutes a significant improvement in the description of solute−solvent interactions, provides us with a means of taking into account a mutual polarization of solute and solvent in a self-consistent way, and allows us to study molecules of complicated, nonspherical shape, and charge distribution. The PCM represents a molecular solute as a quantum mechanical charge distribution contained in a molecular cavity. The cavity is assumed to be immersed in a continuum dielectric. When

SCHEME 1: Structure of Merocyanine Dyes Used in This Manuscript

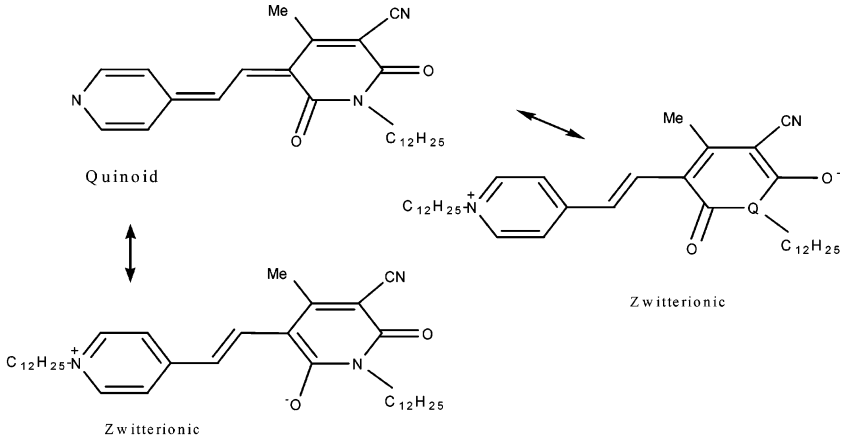

Compound 1

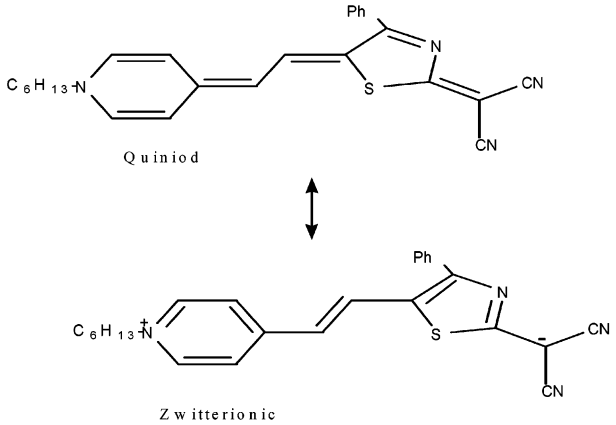

Compound 2

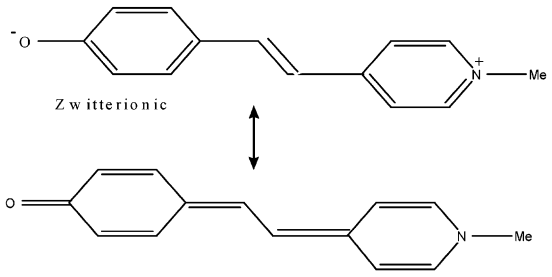

Compound 3

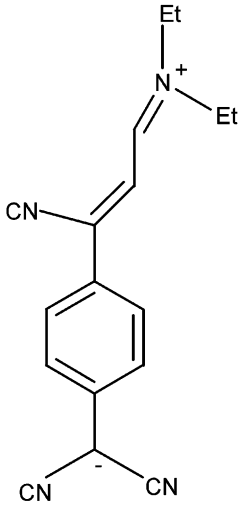

Compound 4.

SCHEME 2: Model Structure of J and H Dimers of Merocyanines

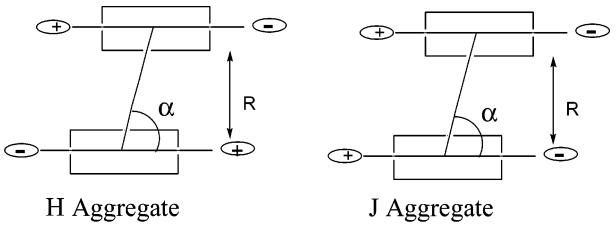

H Aggregate J Aggregate

the dielectric is polarized by the solute, the induced separation of charge gives rise to a response field that modify the previous state of the solute charge distribution. The radius of the molecular-shape cavity used for this DFT/PCM calculation was determined from the molecular length + van der Waals radius of the outermost atoms. In this calculation, we have retained all singly and doubly excited configurations generated from the ground-state Slater determination by considering 20 HOMOs and 20 LUMOs. In TD-DFT/PCM calculation, we reported the norm of the vector part of the β tensor according to

$$\beta_v = (\beta_x^2 + \beta_y^2 + \beta_z^2)^{1/2} \tag{2}$$

where the β_x component can be described by

$$\beta_x = \beta_{xxx} + (\beta_{xyy} + 2\,\beta_{yyx} + \beta_{xzz} + 2\,\beta_{zzx})/3 \tag{3}$$

The optimized ab initio/DFT geometry has been used as an input for TD-DFT/PCM calculation at a photon energy corresponding to 1907 nm.

To calculate dynamic β values of higher aggregates, we have adapted the ZINDO/CV technique combined with SCRF method. The primary code for the ZINDO algorithm was developed by Zerner and co-workers,[44] while the ZINDO/SOS technique has been extensively used by several authors to compute β for different molecules.[45−46] Recently the ZINDO methods has been combined with the correction vector technique to obtain dynamic NLO coefficients in which the sum over all the eigen states of the chosen configuration interaction (CI) Hamiltonian is exactly included.[47−51] We have used this technique to calculate β for the ionic and neutral weak organic acids,[48] and the theoretical values match very well with the experimental data obtained via the HRS technique. The ZINDO calculation of first hyperpolarizabilities follows the correction vector methods as described by Ramasesha et al.[47] In this method, we can obtain the NLO coefficients without resorting to the usual procedure of explicitly solving for a large number of excited states of the CI Hamiltonian, followed by a computation of the transition dipoles among these states. The first-order CV, $\phi_i^{(1)}(\omega)$, is defined by the inhomogeneous linear algebraic equation,

$$(H - E_G + \hbar\omega + i\Gamma)\phi_i^{(1)}(\omega) = \mu_i|G\rangle \tag{4}$$

where **H** is the CI Hamiltonian matrix in the chosen many-body basis, E_G is the ground-state energy, ω is the frequency, $\mu_i = \mu_i = \langle G|\mu_i|G\rangle$ is the ith component of the dipole displacement operator ($i = x, y, z$) and h/Γ is the average lifetime of the excited states. It can be shown that $\phi_i^{(1)}(\omega)$, if expressed in the basis of the eigenstates $\{|R\rangle\}$ of the CI Hamiltonian **H** is given by

$$\Phi_i^{(1)}(\omega) = \sum_R \frac{\langle R|\mu_i|G\rangle}{E_R - E_G + \hbar + i\Gamma}|R\rangle \tag{5}$$

The first-order NLO coefficients can be expressed as

$$\beta_{ijk}(\omega_1,\omega_2) = P_{ijk}\langle\phi_i^{(1)}(-\omega_1 - \omega_2)|\mu_j|\phi_k^{(1)}(-\omega_1)\rangle \tag{6}$$

where the P operators generate all permutations. This method involves solving for the correction vectors in the basis of the configuration functions. The Hamiltonian matrix, dipole matrix, and overlap matrix are usually constructed in the basis of configuration function, in the CI calculation. In this ZINDO/CV calculation, we have retained all singly and doubly excited configurations generated from the ground-state Slater determination by considering 20 HOMOs and 20 LUMOs. The ZINDO/CV calculation of β thus included all the excited states of the Hamiltonian in the restricted CI space. The average β values are then given by

$$\beta^{i}_{av} = \sum_{j=1}^{J=3} {}^1/_3(\beta_{ijj} + \beta_{jji} + \beta_{jij}) \tag{7}$$

To account for the solvent polarity effect in the ZINDO/CV approach, we have used expanded self-consistent reaction field (SCRF) theory[52] where self-consistent solute/solvent interactions are described by dipolar and multipolar terms up to $l = 1-12$. According to this procedure the reaction field R can be defined as

$$R = g_L(\epsilon)\langle\psi|M_{lm}|\psi\rangle \tag{8}$$

where M_{lm} is the moment of the solute charge distribution and the proportional constant g is the modified Onsager factor which can be defined as

$$g_l(\epsilon) = \frac{1}{a^{2l+1}}\frac{(l+1)(\epsilon-1)}{1+\epsilon(1+1)} \tag{9}$$

for $l = 1$ (dipolar term),

$$g(\epsilon) = \frac{2(\epsilon-1)}{(2\epsilon+1)a_0^3} \tag{10}$$

where ϵ is the dielectric constant of the solvent and a_0 is the radius of the spherical cavity. The cavity radius, as used in this ZINDO/CV/SCRF calculation was obtained from the DFT method by calculating the radius, b, from the molecular volume ($=4b^3/3\Pi$) first, and then adding 0.5 Å to account for the nearest approach of the solvent molecules. In other words, a_0 was taken as (b + 0.5) Å. To avoid dispersion effect, we have used photon wavelength corresponding to 1907 nm for computing β tensors. Kanis et al. have shown[45,46] that ZINDO/SCRF can reproduce experimental results in donor−acceptor organic molecules reasonably well. In the above case, we first optimized the geometry at the DFT/PCM level in the presence of appropriate dielectric for different solvents using the Gaussian-03 package. The optimized DFT level geometry is then used as an input for ZINDO/SCRF/CV calculation at a photon wavelength corresponding to 1907 nm. For the dynamic β calculation using TD-DFT/PCM or ZINDO/CV method we have used B convention as discussed by Willetts et al.[53] in detail.

Results and Discussion

Ground-State Geometry, Absorption Maximum, and Exciton Coupling. We have optimized the structure of monomer of merocyanine dyes (Scheme 1) using B3LYP/6-31G** (DFT) levels of theory. To understand the solvent effect in the ground

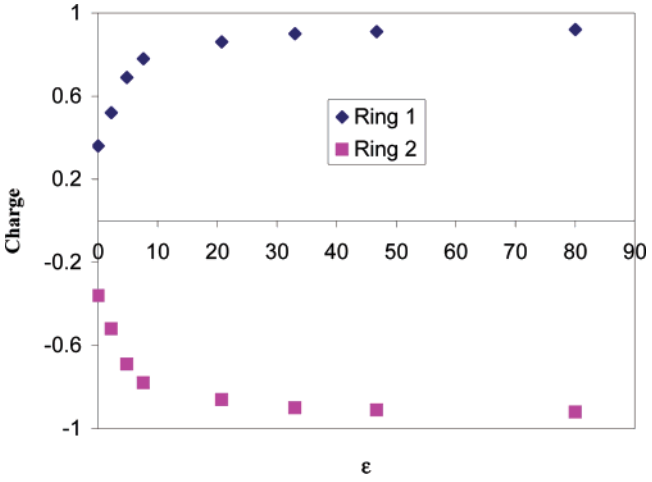

Figure 1. Plot of charge distribution vs ϵ for compound **2** (ring 1 is the pyridine ring and ring 2 is the styryl ring).

state structure, we have optimized the structures with solvent parameters using the PCM scheme. Figure 1 shows the plot of charge distribution vs solvent polarity for compound **2**. Our results clearly show that the structure of compound **2** is dramatically affected by the polarity of the surrounding media. It is interesting to note that the nature of this molecule is predominantly quinoid in the gas phase, and the zwitterionic character is strongly predominant in good polar solvents. An intermediate situation has been found for less polar solvents, such as chloroform. We see the same trend for compounds **1** and **3**.

In the case of the dimer, we have taken the optimized monomer structure as the optimized structure and we varied only intermolecular distance and the slip angle (the angle between the dipole direction and line connecting the two centers). We assumed that the two monomers are stacked coplanar with their transition dipoles exactly antiparallel. The interaction between two monomers in the dimers may be understood using the excitonic coupling model[17,18] based on the point dipole approximation. According this model, due to the dipolar interaction, there will be a splitting of the excited energy levels in the magnitude of

$$\Delta E = 2\mu_{DM}^2/4\pi\epsilon_0 R^3(1 - 3\cos^2\alpha)\sin^3\alpha \qquad (11)$$

where μ_{DM} is the transition dipole-moment, R is the distance between two monomer centers as shown in Scheme 2, and α is the slip angle. To evaluate whether the excitonically coupled monomer model is applicable for mericyanine dimers or not, we carried out a TD-DFT calculation of the electronic transition energies and oscillator strength of the dimer for compound **1**. For the TD-DFT calculation, we have used a DFT optimized monomer structure at the dioxane solvent and then have varied the R from 3.5 to 8 Å with out changing the monomer geometries. At large intermolecular separation, two nearly degenerate electronic transitions are found at around 560 nm (as shown in Figure 2) and these are (1) a forbidden one corresponding to the J transition and (2) a strongly allowed one corresponding to the H transition. The splitting between the forbidden and allowed transitions increases rapidly as the monomers are brought closer and closer. At the distance of around 4.2 Å or less, the splitting between the two lowest transitions begins to increase and the oscillator strength of the H band begins to decrease. The intensity lost from the H-band appears in a new transition shifted more than 3200 cm^{-1} to the blue. This indicates that an excitonically coupled monomer

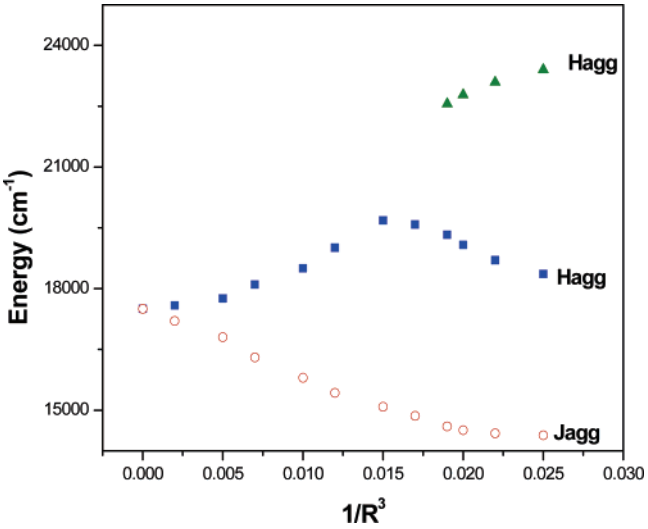

Figure 2. Energies of J and H dimers as a function of the inverse cube of separation between the intermolecular planes.

TABLE 1: Theoretical (T) and Experimental (E) Absorption Maximum (λ_{max}) of Monomer (M), H (Hagg), and J (Jagg) Type Dimers of Merocyanine Dyes in Different Solvents

ϵ	λ^T_M	λ^E_M	λ^T_{Jagg}	λ^E_{Jagg}	λ^T_{Hagg}	λ^E_{Hagg}
2.24	582	593	608		492	506
2.27	572	582	593	604	488	505
4.81	549	558	574		478	489
7.52	543	551	562		473	493
10.42	536	548	551	561	466	492

[a] Experimental data have been taken from ref 23.

picture is reasonable for interplane separations greater than about 4.0 Å but breaks down for shorter distances. We cannot neglect totally the orbital overlap between two monomers at the distances of below 4.0 Å.

To calculate the λ_{max} of H- and J-type dimers (shown in Scheme 2) in different solvents by the TD-DFT method, we have used monomer structure in different solvents as the optimized structure. We used $R = 4.4$ Å and slit angle $= 60°$ for H type dimers, as measured by 2D NMR.[23] In the case of the J-type dimer, we have used the same intermolecular separation and slit angle $= 30°$, as measured in LB films.[24] Table 1 reported the absorption spectra of monomer and both dimers (H and J types) in different solvents. To compare with the reported experimental data we also show the experimental values measured by Wurthner et al.[23] in the same table. Though the calculated values are smaller (3−8%) than the experimental values, the trend of change of λ_{max} with solvent polarity matches very well with the experiment. The J dimer shows the expected shift of the absorption to the red and the H dimer exhibits a blue shift in the absorption band with respect to the monomer. The red shift in the case of the J dimer is due to the dipolar excitonic coupling between two monomers, where as the above coupling canceled mostly in the H dimer due to the antiparallel dipole arrangements between the monomers. Both aggregates exhibited a blue shift in the absorption band as we move toward polar solvents. This is consequence of the higher dipole moments in the ground state than the corresponding excited state for the zwitterionic merocyanine dyes, and as a result the $\Delta\mu$ becomes negative.

First Hyperpolarizabilities of Monomer and Dimers and Effects of Solvent Polarity. Time-dependent density functional theory (TDDFT) has been shown to consistently give accurate excitation energies and oscillator strengths, particularly when

TABLE 2: Dynamic First Hyperpolarizabilities (in 10^{-30} esu) of Compound 4 Calculated Using Different Methods and Compared with Available Experimental Values

optimization method	β calculation method	$CHCl_3$ β	exptl[a]
HF/6-31G**/SCRF	TD-HF/SCRF	−510	
HF/6-31G**/PCM	TD-HF/PCM	−560	
BLYP/6-31G**/SCRF	TD-DFT/SCRF	−890	
BLYP/6-31G**/SCRF	TD-DFT/PCM	−970	780 ± 25
B3LYP/6-31G**/SCRF	TD-DFT/SCRF	−680	
B3LYP/6-31G**/PCM	TD-DFT/PCM	−740	
MP2/6-31G**/SCRF	TD-DFT/SCRF	−710	
MP2/6-31G**/PCM	TD-DFT/PCM	−755	
MP2/6-31G**/SCRF	TD-HF/PCM	−670	

[a] Experimental values have been obtained from *J. Am. Chem. Soc.* **1997**, *119*, 3144. The hyper-Rayleigh scattering method has been used to measure the β values. Since HRS measures $\langle\beta^2\rangle$, one cannot assign the sign of β using the HRS method and that is why experimental β is positive.

employing hybrid exchange correlation function (B3LYP).[54−59] For ground state geometries, we previously found that B3LYP approach is better than HF method for the calculation of the geometry of a host−guest complex whose crystal structure is known. Again, it is well-known that TD-HF lacks important electronic correlations and therefore excited states are symmetrically and significantly blue shifted with respect to the experiment. In contrast, TD-DFT reproduces excited state properties of many systems much better. Particularly TD-B3LYP was found to be very accurate for excited states in many molecular systems.[54−55] This method has already been demonstrated for its accuracy for both linear and nonlinear spectra for different series of substituted chromophores.[56−59] Recently Salek et al.[59] have shown that the hybrid density-functional theory (B3LYP) produces hyperpolarizability results similar to those obtained by coupled-cluster singles-and-doubles theory. To find out which method is good for zwitterionic merocyanine dyes, we have calculated dynamic first hyperpolarizability of compound 4 using optimized structure by HF, MP2, BYLP, and B3LYP methods in the presence of solvents and β's by TD-DFT and TD-HF method at excitation wavelength of 1064 nm and compared with the experimental data (as shown in Table 2) available in the literature.[60] The solvent effect has been taken care using either Onsager's self-consistent reaction field method (SCRF) or polarizable continum model (PCM). Our calculation shows that B3LYP method is much better than BLYP or HF method and is comparable with the MP2 method, which is computationally a costly method even for the monomer. To account for the solvent effect, the PCM model is much better than the Onsager reaction field method (as we can see from Table 2), and several publications [38−39,41−43] have noted the same trend for the solvent effect and discussed the details about the superiority of the former. Though PCM is a nonpolar model, it has been shown in several publications[61−63] that PCM can reproduce experimental results in polar media. Francesa et al.[61] have shown that solvation dynamics of ionic coumarine dyes in acetonitrile solvent using the PCM model matches well with molecular dynamics (MD) simulation results. Jonna et al.[62] have reported that the PCM model can calculate the acid−base equilibria of substituted phenols in acetonitrile solvent, and it matched well the experimental values. Benedetta et al.[63] have shown that PCM model can reproduce experimental transtion energies for 4-(*N*,*N*-dimethylamino)benzonitrile in different polar solvents. Our calculations (as shown in Table 2) also show that PCM can reproduce experimental first hyperpolarizabilities for zwitterionic dyes. Here we calculate the first hyperpolarizabilities of monomers and H- and J-type dimers (as shown in Scheme 2) in different solvents by the TD-DFT/SOS method using solvent parameters and 1907 nm as excitation source. We have used B3LYP/PCM optimized monomer structure in different solvents as the optimized structure, and the monomers are separated by 4.4 Å. The slit angle was kept as 60° for H-type dimers and at 30° for J-type dimers. Computed β values in dichloromethane solvent are shown in Table 3. For a given solvent the first hyperpolarizability of the J-type dimer is 1.4−1.8 times higher than the corresponding monomer, whereas β's for H-type dimer are 2.5−3.5 times lower than those for the corresponding monomer. The origin of the change in hyperpolarizabilities in zwitterionic monomers to J- and H-type dimers can be explained using the two-state model. According to the two-state model[33]

TABLE 3: First Hyperpolarizabilities of Monomer and Aggregates at Dichloromethane Solvents

compound	β^{monomer}	$\beta^{\text{J-aggregate}}$	$\beta^{\text{H-aggregate}}$
1	−540	−970	−194
2	−445	−720	−142
3	−280	−476	−91

$$\beta^{\text{two-state}} = \underbrace{\frac{3\,\mu_{eg}^{\,2}\,\Delta m_{eg}}{E_{eg}^{\,2}}}_{\text{static factor}} \underbrace{\frac{\omega_{eg}^{\,2}}{(1-4\omega^2/\omega_{eg}^{\,2})\,(\omega_{eg}^{\,2}-\omega^2)}}_{\text{dispersion factor}} \quad (12)$$

where μ_{eg} is the transition dipole moment between the ground state $|g\rangle$ and the charge-transfer excited state $|e\rangle$, $\Delta\mu_{eg}$ is the difference in dipole moment, and E_{eg} is the transition energy. Our calculation indicate that in the case of the J-type of dimers, the increment of first hyperpolarizability is due to two factors and these are (1) the red shift of the absorption maxima, which brings it closer to the peak of the two-photon resonance wavelength and (2) $\Delta\mu_{eg}$ values are about 1.2−1.5 times those of the corresponding monomer. Similarly, in the case of the H-type of dimer due to the antiparallel dipoles, the hyperpolarizabilities were greatly reduced, and this can be due to several factors including (1) the blue shift of absorption maximum and 2) $\Delta\mu_{eg}$ values are 2−3 times lower than those for the corresponding monomer. Our calculations indicate that the electrostatic aggregation of merocyanine dyes is very important for the limit of the performance of the electrooptic properties at higher dye level loading. Generally it has been assumed that the formation of nearly centrosymmetric aggregates prevents the effect poling in the presence of an applied electric field. Our result shows that the first hyperpolarizability itself changes tremendously with the aggregation, and it can be a very important factor for the poor performance at higher dye concentration. First hyperpolarizabilities for the H-type of dimer are about three times lower than that for the corresponding monomer. So it will reduce the material bulk succeptibility three times further than expected due to the hindered electric field poling, whereas J aggregation can enhance the effective $\chi(2)$ as it simultaneously increases the molecular hyperpolarizability and also produces a larger ground-state dipole moment, which should improve the order parameter of the poling process.

Our calculation shows a remarkable solvent effect on the first hyperpolarizabilities of zwitterionic monomers as well as dimers. Figure 3 shows the variation of β's with solvent dielectric constant for compound **2**. Changing the solvent from low to high dielectric causes not only an increase in magnitude of β but also a change in sign, therefore causing the curve to pass through zero at intermediate dielectric. In both cases (monomer and dimers), the first order NLO responses are low and positive

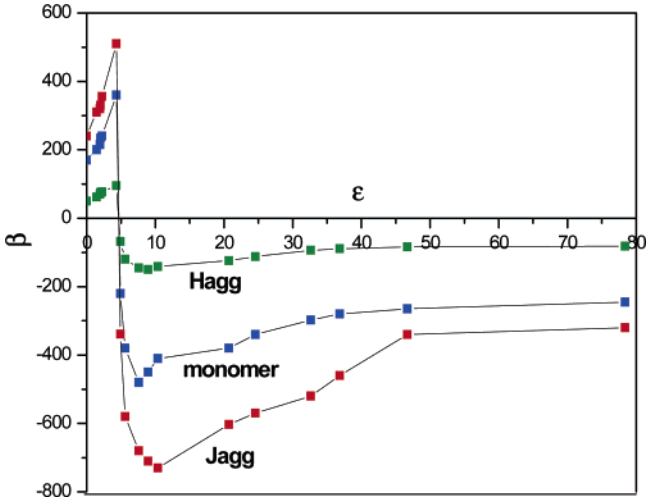

Figure 3. β vs ϵ for monomer, H and J-Type dimers of compound **2**.

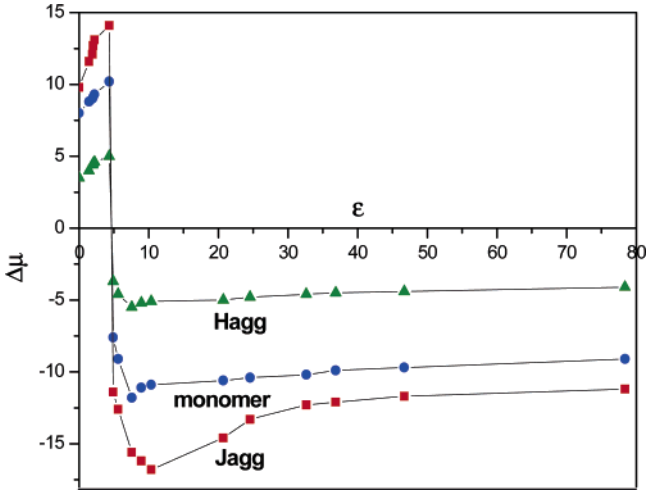

Figure 4. $\Delta\mu$ vs ϵ for monomer, H and J-type dimers of compound **2**.

in the gas phase and then increase slowly with solvent polarity. Then it started to decrease with the solvent polarity. The β values remain negative in all the polar solvents and pause highest values at a moderate ϵ (8−10) and then again decrease slowly with the increase of ϵ. This behavior is mainly due to the change of the structure of monomer from quinoid to zwitterionic form. Once it is in mostly zwitterionic form, β values decrease with the increase of solvent polarity. Same picture is valid for compounds **1** and **3** also. Recently the same type of behavior for zwitterionic monomers have been observed experimentally by Abbotto et al.[64−65] So there are clearly important consequences from this, in choice of solvent and molecular environment when evaluating NLO molecules of merocyanine monomers and aggregates. An excellent NLO response in solution might vanish when the active chromophore is dispersed in a matrix with suitable ϵ. The same chromophore can prove to perform very well under an appropriately chosen solvent. The commonly established procedure for the NLO compound to report β values in one solvent may in certain cases be insufficient to draw definite conclusions on the overall chromophore performance and the prospect for different design strategies.

To understand the origin of the remarkable solvent effects in zwitterionic monomers and dimers, we calculated the change in dipole moment between ground and charge-transfer excited state ($\Delta\mu_{eg}$). Since μ_{eg}^2 and E_{eg}^2 cannot be negative, according to the two-state model, β will be negative only if $\Delta\mu_{eg}$ is negative. Figure 4 shows the plot of the $\Delta\mu_{eg}$ vs ϵ for monomer and dimers at different solvents. It is interesting to note that the trend in the variation of $\Delta\mu_{eg}$ and β with ϵ is quite similar, which follows two-state model perfectly. This confirms that the $\Delta\mu_{eg}$ could be the main factor for the remarkable solvent effect on the first hyperpolarizabilities of the zwitterionic molecules.

Dimers are only a first approximation to the aggregates present in real materials. In real chromophore−polymer system at higher chromophore loading, the chrmophore may exist in a wide range of forms including monomers, various types of dimers, higher aggregates and large nano or microcrystalline states. Higher aggregates of highly dipolar push−pull chromophores are recognized to limit the performance of electrooptic and other nonlinear optical effects that require loading of a higher concentration chromophore into a polymer. So it is very important to understand how the β's vary with the increase in number of monomers in both J and H aggregates. Since a very high computational cost is required to calculate the dynamic β's for higher aggregates using TD-DFT/SOS approach, here we have investigated the dynamic hyperpolarizabilities of higher

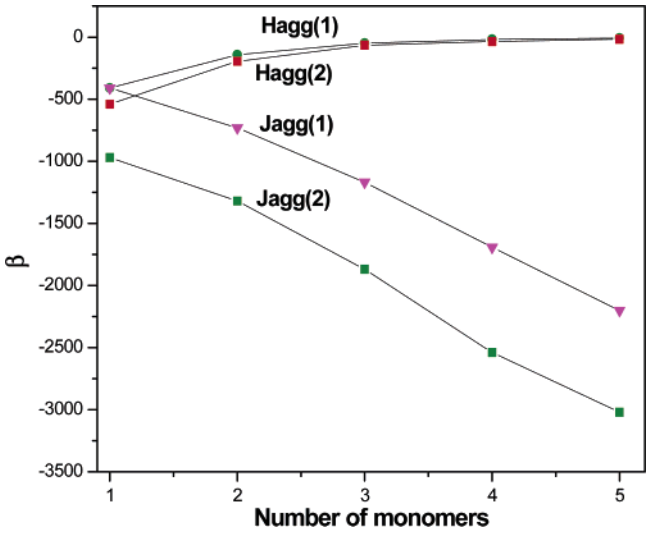

Figure 5. Plot of β vs the number of monomers in the H- and J-type aggregates for compounds **1** and **2**.

aggregates at $\epsilon = 10.36$, using ZINDO/CV/SCRF method and 1907 nm as excitation source. In the case of higher aggregates, we have taken DFT optimized monomer structure using solvent dielectric constant $\epsilon = 10.36$, as optimized structure and the monomers are separated by 4.4 Å to each other. The slit angle kept as 60° between two consecutive monomer for H-type aggregates and 30° for J-type aggregates. Figure 5 shows how the first hyperpolarizabilities change with the number of monomers in the aggregates for compounds **1** and **2**.

Our calculations indicate that the β values for J-type aggregates increase tremendously from −410 (for monomer) to to −2201 for pentamer in the case of compound **2**, whereas the first hyperpolarizabilities decrease to −7 for pentamer in the case of H-type aggregates. The same trends have been observed for compounds **1** and **3**. This can explain the recent observation of drastic change in first hyperpolarizabilities with concentration by Cross et al.[32] As we discussed before, the merocyanine dyes are known to form H-type aggregates mainly in nonpolar solvents. Cross et al.[32] has performed the EFISHG experiment in the concentration range 10^{-3}−10^{-1} M. With the increase of concentration from 10^{-3} to 10^{-1} M one can expect the formation of higher H-type aggregates. Since the β values decrease tremendously with the increase of number of monomers in the aggregates, one can expect the total β values will be near zero at higher concentration. In the EFISHG experiment the

second harmonic intensity, $I_{2\omega}$, is proportional to ($\gamma + \mu\beta$/5KT). One cannot measure accurate $\mu\beta$ values from EFISHG experiment with out knowing the γ values of monomer and aggregates. So the small positive values of $\mu\beta$'s have been observed by Cross et al.[32] at higher concentration can originate from electronic induced second harmonic nonlinearity of monomers and aggregates via the third-order electronic suceeptibility as discussed by Cross et al.[32]

Conclusion

In this paper, we have reported the first hyperpolarizabilities of monomer and aggregates of zwitterionic merocyanine chromophores. We have analyzed a variety of effects on the β values for zwitterionic monomers and aggregates. We have demonstrated that the dynamic hyperpolarizabilities of J-type aggregates are several times higher than that of monomers, and this is due to the fact that (1) the red shift of the absorption maxima, which brings it closer to the peak of the two-photon resonance wavelength, and (2) $\Delta\mu_{eg}$ values for dimers are about 1.2−1.5 times lower than those of the corresponding monomer. However, the hyperpolarizability reduces tremendously for the H-type of aggregates due to the antiparallel dipoles, and this can be due fact that (1) the blue shift of the absorption maximum and (2) $\Delta\mu_{eg}$ values for dimers are 2−3 times lower than those for the corresponding monomer. We find that the solvent effects are really impressive for merocyanine monomers and aggregates. An excellent NLO response in solution might vanish when the active chromophore is dispersed in a matrix with suitable ϵ. The commonly established procedure for the NLO compound to report β values in one solvent may in certain cases be insufficient to draw definite conclusions on the overall chromophore performance and the prospect for different design strategies. In aggregates, a large number of chromophores together with large number of solvents are involved, so one needs to include all the aggregates and solvents in the calculation in order to find the macroscopic aggregation effect. Since taking large number of aggregates and solvents together is not feasible using quantum chemical calculations, our result can be used as a model for experimental observation but not for the exact experimental values for aggregates in a macroscopic device system.

Acknowledgment. We thank the Mississippi Center for Super Computer Resource (MCSR), University of Mississippi, Oxford, MS, for the generous use of their computational facilities. We also thank reviewers whose valuable suggestion improved the quality of the manuscript.

References and Notes

(1) Zyss, J. *Molecular Nonlinear Optics: Materials, Physics and Devices*; Academic Press: New York, 1994.

(2) Nalwa, H. S.; Miyata, S. *Nonlinear Optics of Organic Molecules and Polymers*; CRC Press: Boca Raton, FL, 1997.

(3) Mkuzyk, M. G. Nonlinear Optical Properties of Organic Materials. *SPIE Proc.* **1997**, 3147.

(4) Marder, S. R.; Perry, J. W.; Schaefer, P. W. *Science* **1989**, *245*, 626.

(5) Clays, K.; Wostyn, K.; Olbrechtes, G.; Persoons, A.; Watanabe, A.; Nogi, K.; Duan, X.-M.; Okada, S.; Oikawa, H.; Nakanishi, H.; Bredas, J. L. *J. Opt. Soc. Am. B.* **2000**, *17*, 256.

(6) Clays, K.; Coe, B. *J. Chem. Mater.* **2003**, *15*, 642.

(7) Coe, B. J.; Jones, L. A.; Harrs, J. A.; Brunschwig, B. S.; Asselberghs, I.; Clays, K.; Persoons, A. *J. Am. Chem. Soc.* **2003**, *125*, 862.

(8) Coe, B. J.; Jones, L. A.; Harrs, J. A.; Brunschwig, B. S.; Asselberghs, I.; Clays, K.; Persoons, A.; Garin, J.; Orduna, J. *J. Am. Chem. Soc.* **2004**, *126*, 3880.

(9) Burland, D. M.; Miller, R. D.; Walsh. C. A. *Chem. Rev.* **1994**, *94*, 31.

(10) Dalton, L. R.; Harper, A. W.; Robinson, B. H. *Proc. Natl. Acad. Sci. U. S.A.* **1997**, *94*, 4842.

(11) Shi, Y.; Zhang, C.; Zhang, H.; Bechtel, J. H.; Dalton, L. R.; Robinson, B. H.; Steir, W. H. *Science* **2001**, *288*, 119.

(12) Wu, X.; Wu, J.; Jen, A. K. Y. *J. Am. Chem. Soc.* **1999**, *121*, 472.

(13) Dorr, M.; Zentel, R.; Dietrich, R.; Meerholz, K.; Brauchle, R.; Wichern, J.; Boldt. P. *Macromolecules* **1998**, *31*, 1454.

(14) Liakatas, A.; Cai, M.; Bosch, M.; Jager, C.; Bosshard, P.; Gunter, P.; Zhang, C.; Dalton, L. R. *Appl. Phys. Lett.* **2000**, *76*, 1368.

(15) Yitzchaik, S.; Di Bella, S.; Lundquist, P. M.; Wong, G. K.; Marks, T. J. *J. Am. Chem. Soc.* **1997**, *119*, 2995.

(16) Di Bella, S.; Fragala, I.; Narks, T. J.; Ratner, M. A. *J. Am. Chem. Soc.* **1996**, *118*, 12747.

(17) Davydov, A. S. *Theory of Molecular Excitation*; McGraw-Hill: New York, 1962.

(18) Mccullough, J. *Chem. Rev.* **1987**, *87*, 811.

(19) Yartsev, V. M.; Singh, M. R. *Chem. Phys.* **2002**, *276*, 293.

(20) Di Bella, S.; Lanza, G.; Fragaia, I.; Yitzchaik, S.; Ratner, M. A.; Marks, T. J. *J. Am. Chem. Soc.* **1997**, *119*, 3003.

(21) Datta, A.; Pati, S. K. *J. Chem. Phys.* **2003**, *118*, 8420.

(22) Gullaume, M.; Botek, E.; Champagne, B.; Caster, F.; Ducasse, L. *J. Chem. Phys.* **2004**, *121*, 7390.

(23) Wurthner, F.; Yao, S.; Debaerdemaeker, T.; Wortmenn, R. *J. Am. Chem. Soc.* **2002**, *124*, 9431.

(24) Ikegami, K. *J. Chem. Phys.* **2004**, *121*, 2337.

(25) Clays, K.; Persoons, A. *Phys. Rev. Lett.* **1991**, *66*, 2980.

(26) Ray, P. C.; Das, P. K. *J. Phys. Chem.* **1995**, *99*, 14414.

(27) Maeder, S. R.; Gormann, C. B.; Meyers, F.; Perry, J. W.; Bourhill, G.; Bredas, J. L.; Pierce, B. M. *Science* **1994**, *265*, 632.

(28) Maeder, S. R.; Gormann, C. B.; Tienmann, B. G.; Cheng, L. T. *J. Am. Chem. Soc.* **1993**, *115*, 3006.

(29) Minken, I. V. *Chem. Rev.* **2004**, *104*, 2751.

(30) Morly, J. O.; Morley, R. A.; Fitton, L. A. *J. Am. Chem. Soc.* **1998**, *68*, 1295.

(31) Champgne, B.; Legrand, T.; Perple, E. A.; Quinet, O.; Andre, J. M. *Collect. Czech. Chem. Commun.* **1998**, *68*, 1295.

(32) Cross, G. H.; Hackman, N. A.; Thomas, P. R.; Szablewski, M.; Palsson, L. O.; Bloor, D. *Opt. Mater.* **2002**, *21*, 29.

(33) Oudar, J. L. *J. Chem. Phys.* **1977**, *67*, 446.

(34) Runge, E.; Gross, E. K. U. *Phys. Rev. Lett.* **1984**, *52*, 997.

(35) Van Leeuwen, R. *Int. J. Mod. Phys., B* **2001**, *15*, 1969.

(36) Jensen, L.; Van Duijnen, P. T.; Snijders, J. G. *J. Chem. Phys.* **2003**, *119*, 12998.

(37) Van Gisbergen, P. T.; Snijders, J. G.; Baerends, E. J. *J. Chem. Phys.* **1998**, *109*, 10644.

(38) Miertus, S.; Scrocco, E.; Tomassi, J. *J. Chem. Phys.* **1981**, *55*, 117.

(39) Cammi, R.; Tomassi, J. *J. Comput. Chem.* **1995**, *16*, 1449.

(40) Gaussian 03, Revision A 9. Frisch, M. I.; Trucks, G. W.; Schlegel, H. B.; Pople, J. A. Gaussian Inc.: Pittsburgh PA, 2003.

(41) Cammi, R.; Menucci, B.; Tomasi, J. *J. Phys. Chem. A.* **2000**, *104*, 4690.

(42) Luo, Y.; Norman, P.; Macak, P.; Agren, H. *J. Chem. Phys.* **1999**, *111*, 9853.

(43) Mennucci, B.; Tomasi, J. *J. Chem. Phys.* **1997**, *106*, 5151.

(44) Kotzian, M.; Rosch, N.; Schroder, H.; Zerner, M. C. *J. Am. Chem. Soc.* **1989**, *111*, 7687.

(45) Kanis, D. R.; Ratner, M. A.; Marks, T. J. *J. Am. Chem. Soc.* **1993**, *115*, 1078.

(46) Kanis, D. R.; Lacroix, P. G.; Ratner, M. A.; Marks, T. J. *J. Am. Chem. Soc.* **1994**, *116*, 10089.

(47) Ramasesha, S.; Shuai, Z.; Bredas, J. L. *Chem. Phys. Lett.* **1995**, *245*, 226.

(48) Ray, P. C.; Ramasesha, S.; Das, P. K, *J. Chem. Phys.* **1996**, *105*, 9633.

(49) Ray, P. C. *Chem. Phys. Lett.* **2004**, *394*, 354.

(50) Ray, P. C. *Chem. Phys. Lett.* **2004**, *395*, 269.

(51) Ray, P. C.; Leszczynski, J. *Chem. Phys. Lett.* **2004**, *399*, 162.

(52) Rivali, J. L.; Rinaldi, D. *Chem. Phys.* **1976**, *18*, 233.

(53) Willetts, A.; Rice, J. E.; Burland, D. M. *J. Chem. Phys.* **1992**, *97*, 7590.

(54) Furche, F.; Ahlrichs, R. *J. Chem. Phys.* **2002**, *117*, 7433.

(55) Onida, G.; Reining, L.; Rubio, A. *Rev. Mod. Phys.* **2002**, *74*, 601.

(56) Masonuv, A.; Tretiak, S. *J. Phys. Chem. B* **2004**, *108*, 899.

(57) Bartholomew, G. P.; Rumi, M.; Pond, S. J.; Perry, J. W.; Tretiak, S.; Bazan, G. C. *J. Am. Chem. Soc.* **2004**, *126*, 11529.

(58) Day, P. N.; Naguyen, K. A.; Pachter, R. *J. Phys. Chem. B* **2005**, *109*, 1803.

(59) Salek, P.; Helgaker, T.; Vahtras, O.; Agren, H.; Jossons, D.; Gauss, J. *Mol. Phys.* **2005**, *103*, 439.

(60) Szblewski, M.; Thomas, P. R.; Thornton, A.; Bloor, D.; Cross, G. H.; Cole, J. M.; Howard, A. K. J.; Malagoli, M.; Meyers, M.; Bredas, J. L.; Goovaerts, E. *J. Am. Chem. Soc.* **1997**, *119*, 3144.

(61) Francesca, I.; Branka, M. L.; Benedatta, M.; Dolores, M. E.; Tomasi, J. *J. Phys. Chem. B.* **2005**, *109*, 3553.

(62) Jonna, M.; Mariusz, M.; Lech, C. *J. Phys. Chem. A* **2004**, *108*, 10354.

(63) Benedetta, M.; Alessandro, T.; Jacopo, T. *J. Am. Chem. Soc.* **2000**, *122*, 10621.

(64) Abbotto, A.; Bradamante, S.; Facchetti, A.; Pagani, G. A.; Ledoux, I.; Zyss, J. *Metr. Res. Soc. Symp. Soc.* **1998**, *488*, 819.

(65) Abbotto, A.; Beverina, L.; Bradamante, S.; Facchetti, A.; Klein, C.; Pagani, G. A.; Wortmann, R. *Chem.—Eur. J.* **2003**, *9*, 1991.